Electronic Supplementary Material (ESI) for Inorganic Chemistry Frontiers.
This journal is © the Partner Organisations 2019

Electronic Supplementary Information

Ni/Fe-based Heterometallic Phthalocyanine Conjugated Polymer for Oxygen Evolution Reaction

Dongdong Qi,[#] Xin Chen,[#] Wenping Liu,[#,*] Chenxi Liu, Wenbo Liu, Kang Wang,*

and Jianzhuang Jiang*

Experimental Section

General Remarks: THF and Et_3N were distilled from Na and CaH_2, respectively. All other reagents and solvents were reagent grade and used as received. The compounds $Fe[Pc(I)_4]$,[S1] $Fe[Pc(ethynyl)_4]$,[S1] $Ni[Pc(I)_4]$,[S1] $Ni[Pc(ethynyl)_4]$,[S1] and FePc-CP[S1] were prepared according published procedures. All coupling reactions were carried out under a nitrogen atmosphere.

IR spectra were recorded as KBr pellets using a Bruker Tensor 37 spectrometer with 2 cm^{-1} resolution. PXRD data were collected on a Shimadzu XRD-6000 diffractometer using Cu-K*a* radiation (I = 1.54056 Å) at room temperature. SEM images were obtained using a JEOL JEM-6510A scanning electron microscopy. For SEM imaging, a drop of freshly prepared sample dispersion was cast onto a silicon slice, and then Au (1-2 nm) was sputtered onto the grids to prevent charging effects and to improve the image clarity. TEM images were measured by a JEOL JEM-2200FS electron microscope. HAADF-STEM images and EDS mapping images were taken on a JEM-ARM200F electron microscope operated at 200 kV. The Fe and Ni contents of $Fe_{0.5}Ni_{0.5}$Pc-CP, NiPc-CP, and FePc-CP were determined by ICP-AES analysis with an IRIS Intrepid II XRP instrument. XPS was carried out on PHI 5300 ESCA System (PerkineElmer, USA). Solid-state UV-Vis diffuse reflectance spectra were recorded on an SHIMADZU UV-2600 spectrophotometer. TGA was performed on a PerkinElmer TG-7 analyzer with a heating rate of 10 °C min^{-1} in the range of 25-900 °C under N_2 atmosphere.

Synthesis of $Fe_{0.5}Ni_{0.5}$Pc-CP: A mixture of Fe[Pc(I)$_4$] (128 mg, 0.12 mmol) and Ni[Pc(ethynyl)$_4$] (80 mg, 0.12 mmol) in a mixed solvent of Et_3N (20 ml) and THF (10 ml) in the presence of catalysts $Pd(PPh_3)_2Cl_2$ (2.8 mg,14.7 μmol) and CuI (0.74 mg, 3.6 μmol) was heated to 70°C for 48 h under N_2 atmosphere. After the mixture was cooled to room temperature, the precipitate was filtered and washed with THF, toluene, and methanol to remove any phthalocyanine monomers and catalysts. The product was dried at 80°C under vacuum for 12 h to yield $Fe_{0.5}Ni_{0.5}$Pc-CP as a dark blue powder (0.19 g, yield 92%). The Fe and Ni content were 2.94 and 3.82 wt%, respectively, as determined by ICP-AES.

Synthesis of NiPc-CP： By employing the above-described procedure for the synthesis of $Fe_{0.5}Ni_{0.5}$Pc-CP with Ni[Pc(I)$_4$] instead of Fe[Pc(I)$_4$] as starting material, NiPc-CP was isolated in the yield of 93%. The Ni content was 6.34 wt% as determined by ICP-AES.

Preparation of the working electrode: The catalyst ink was prepared by dispersing 4 mg of sample into 0.75 mL ethanol and 0.25 mL deionized water solvent containing 5 μL of 5 wt% Nafion and sonicated for 60 min. Then, 5.0 μL of the mixture was dropped onto a polished glassy carbon electrode (4 mm in diameter). The loaded electrode was placed in a 60 C oven for 10 min to dry and then was taken out to cool down before all the tests. The corresponding catalyst loading is 0.16 mg cm^{-2}.

Electrochemical Measurements. The electrochemical measurements were conducted on the CHI 760E workstation (CH Instruments, Inc.) with a RRDE-3A rotator (ALS Co., Ltd). The typical three-electrode system was employed to evaluate the electrochemical properties of the prepared catalysts. Specifically, glassy carbon was the working electrode, a Pt wire was the counter electrode, and the Ag/AgCl (in saturated KCl solution) was the reference electrode. All potentials were referred to the reversible hydrogen electrode by adding a value of (0.197 + 0.059×pH) V. For OER tests, first of all, the electrochemical accessibility of the working electrode was optimized by potential cycling between 1.1 and 1.6 V vs. RHE at 50 mV s^{-1} in 1.0 M KOH until the system became stable. LSV was carried out at the scan rate of 10 mV s^{-1} with the rotating speed of 1600 rpm. All the electrochemical tests in this study were conducted at least three times to ensure the accuracy of the measurements. Besides, the iR correction was applied to get rid of the influence of the Ohmic resistance.

iR-Correction. The iR correction has been adopted to remove the influence of Ohmic resistance on the OER measurements. Specifically, the electrochemical alternating current impedance spectroscopy (EIS) was utilized to measure the Ohmic resistance under the OER conditions. The potentials were calculated *via* the following equation:

$$E_{\text{iR-corrected}} = E - iR$$

Where i is the current, R is the uncompensated ohmic electrolyte resistance measured *via* high frequency A.C. impedance in 1.0 M KOH solution, which is around 11 Ω for all the tested samples.

Determination of turnover frequency (TOF). The TOF can be calculated by the following equations.

$$TOF = \frac{I}{2Fn}$$

Here, I is the current during the linear sweep measurement (in A), F is the Faraday constant (in C mol^{-1}), n is the number of actives sites (in mol). The factor 1/4 suggests that the formation of one oxygen molecule needs four electrons.

Theoretical Caculation. Based on the experimental results, the higher catalytic activity of the heterometallic conjugated network $Fe_{0.5}Ni_{0.5}$Pc-CP originates from the synergistic effect between the proximate Fe and Ni ions. In an attempt to understand the synergistic effect, density functional theory (DFT) calculations were carried out at the level of B3LYP-GD3//SDD/6-311++G(2d,p)/6-311G(d)[S2-S4]. Three computational configuration, including FePc≡NiPc, FePc≡FePc, and NiPc≡NiPc, were derived from the basic structural units of $Fe_{0.5}Ni_{0.5}$Pc-CP, FePc-CP, and NiPc-CP. Clearly, the metal ions are the active sites for the OER in all the three models. For all the four models, the 4e^{-} oxygen evolution reaction in alkaline condition proceeds along the following pathways (* denotes active site):

$$M^{*} + OH^{-} \rightarrow MOH^{*} + e^{-} \qquad (1)$$

$$MOH^{*} + OH^{-} \rightarrow MO^{*} + H_2O_{(l)} + e^{-} \qquad (2)$$

$$MO^{*} + OH^{-} \rightarrow MOOH^{*} + e^{-} \qquad (3)$$

$$MOOH^{*} + OH^{-} \rightarrow M^{*} + O_{2(g)} + H_2O_{(l)} + e^{-} \qquad (4)$$

The reaction free energy (ΔG) is calculated by this formula

$$\Delta G = \Delta H - T\Delta S - qU + k_B T ln10 \times pH$$

Here ΔH is the reaction enthalpy of an elementary electron transfer step in

OER and is estimated by the reaction energy (ΔE) with zero-point energy (ZPE) correction from DFT calculations; $T\Delta S$ is the contribution in free energy changes from entropy; U is the applied potential in electrode; q is the charge transfer in each step.

.

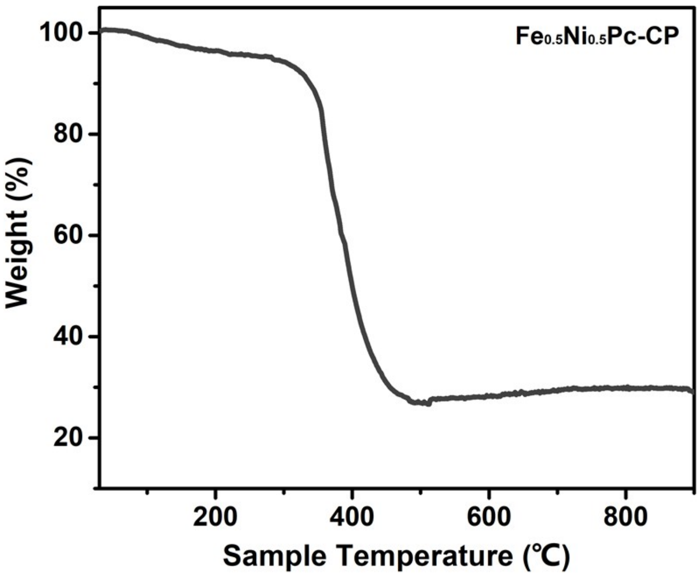

Fig. S1 TGA of $Fe_{0.5}Ni_{0.5}$Pc-CP.

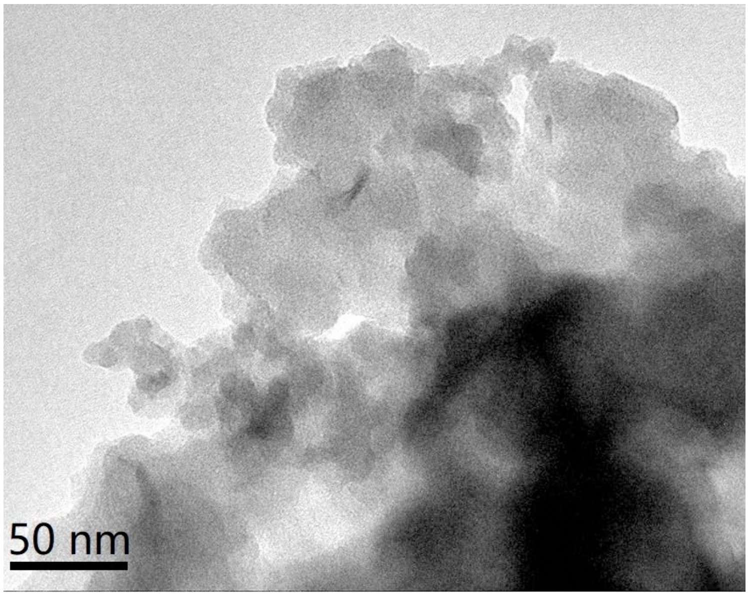

Fig. S2 TEM image of $Fe_{0.5}Ni_{0.5}$Pc-CP.

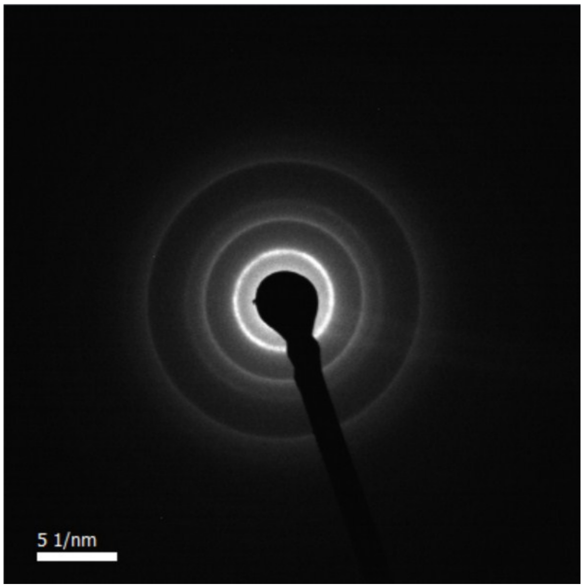

Fig. S3 SAED pattern of $Fe_{0.5}Ni_{0.5}$Pc-CP.

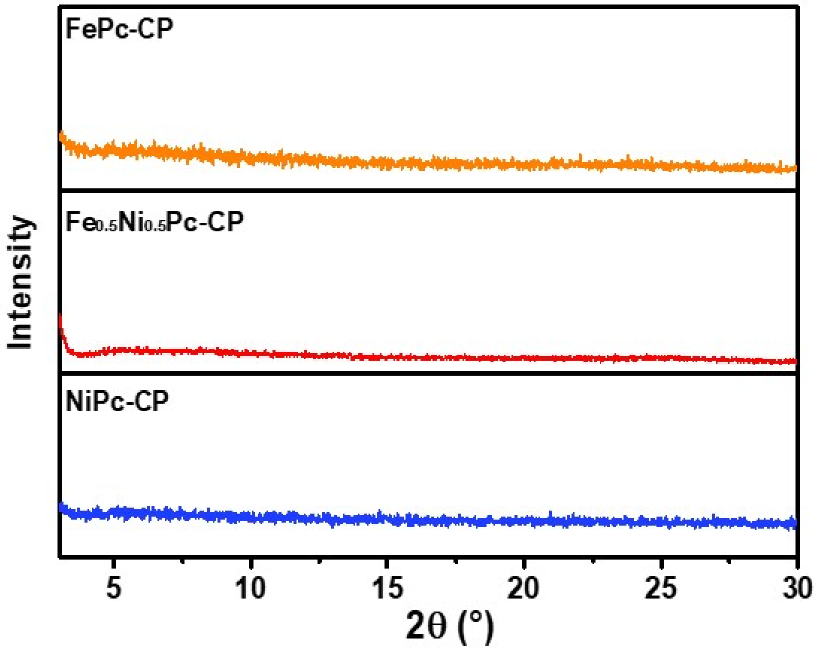

Fig. S4 PXRD patterns of FePc-CP, $Fe_{0.5}Ni_{0.5}$Pc-CP, and NiPc-CP.

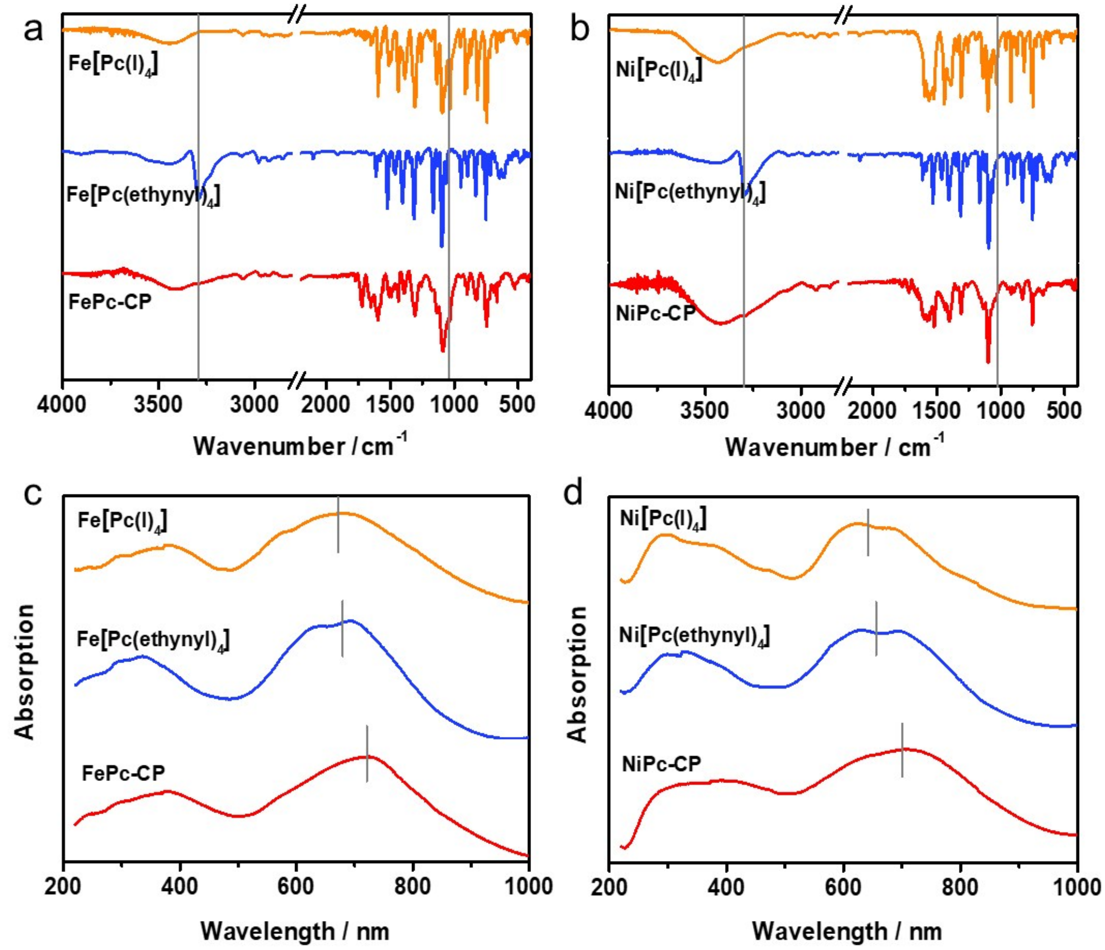

Fig. S5 (a) FT-IR and (c) solid-state UV-vis diffuse reflectance spectra of FePc-CP and corresponding phthalocyanine monomers. (c) FT-IR and (d) Solid-state UV-vis diffuse reflectance spectra of NiPc-CP and corresponding phthalocyanine monomers.

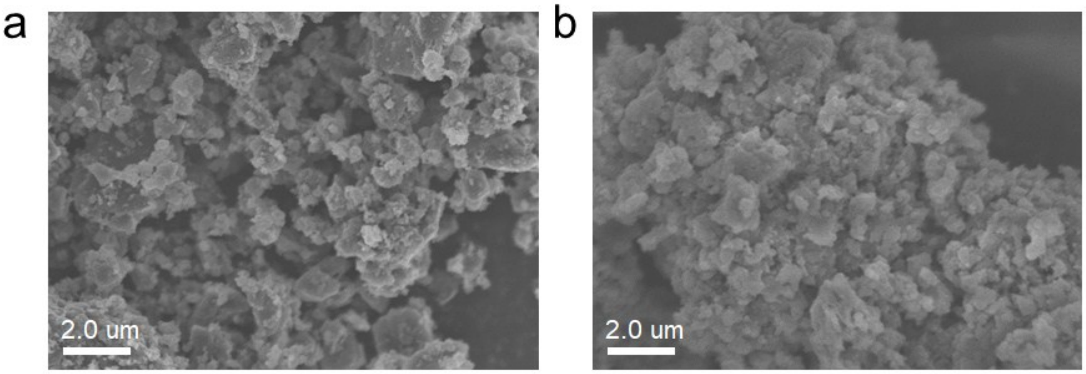

Fig. S6 SEM images of (a) FePc-CP and (b) NiPc-CP.

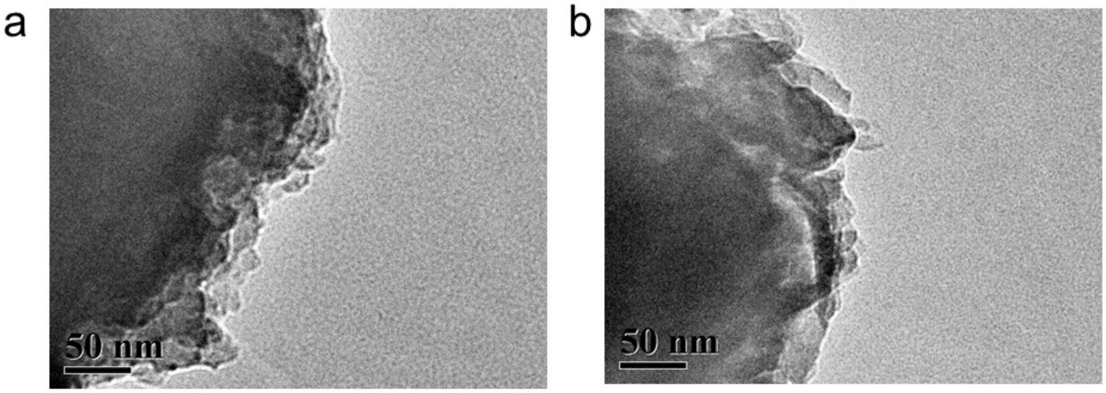

Fig. S7 TEM images of (a) FePc-CP and (b) NiPc-CP.

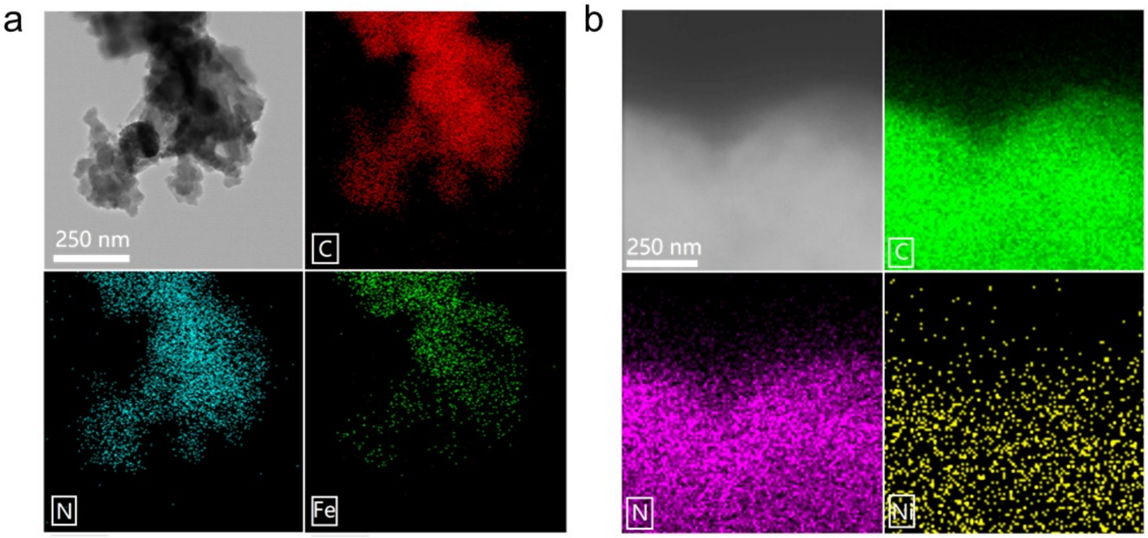

Fig. S8 The STEM and elemental-mapping images of (a) FePc-CP and (b) NiPc-CP.

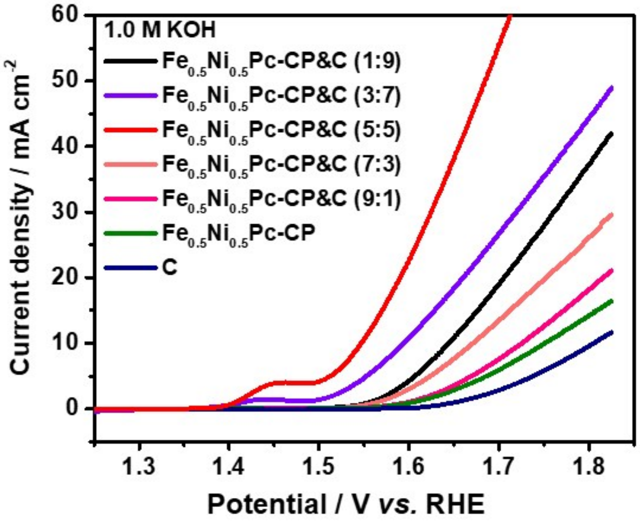

Fig. S9 LSV curves of pure XC-72 and $Fe_{0.5}Ni_{0.5}Pc$-CP mixture with different contents measured at the scan rate of 10 mV s^{-1} with the rotation speed of 1600 rpm in 1.0 M KOH solution.

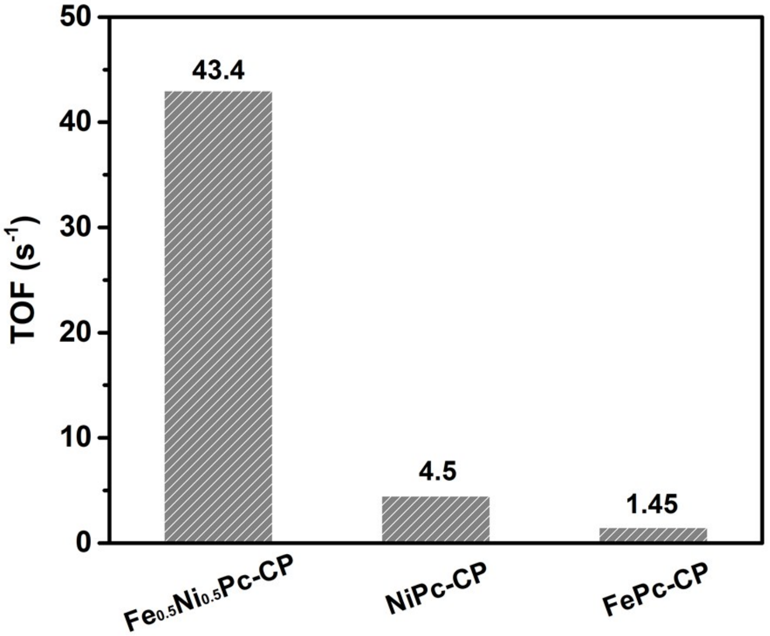

Fig. S10 Turnover frequency (TOF) of FePc-CP, FePc-CP, and $Fe_{0.5}Ni_{0.5}$Pc-CP at the overpotential of 317 mV.

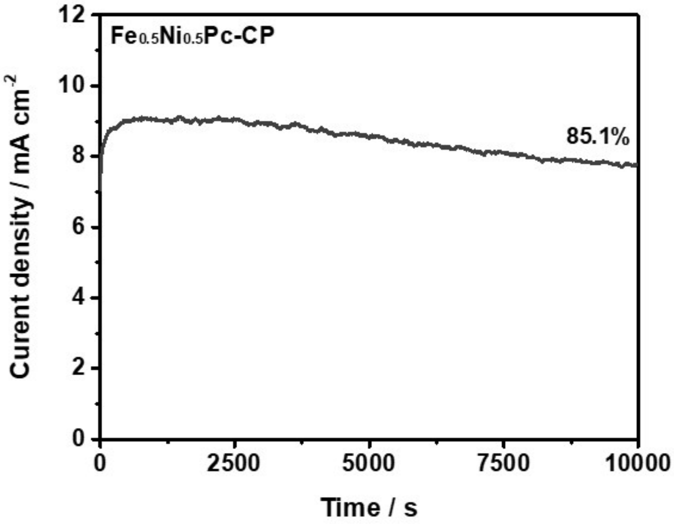

Fig. S11 Amperometric i–t curve of $Fe_{0.5}Ni_{0.5}$Pc-CP-modified electrode tested with the rotation speed of 1600 rpm in 1.0 M KOH solution.

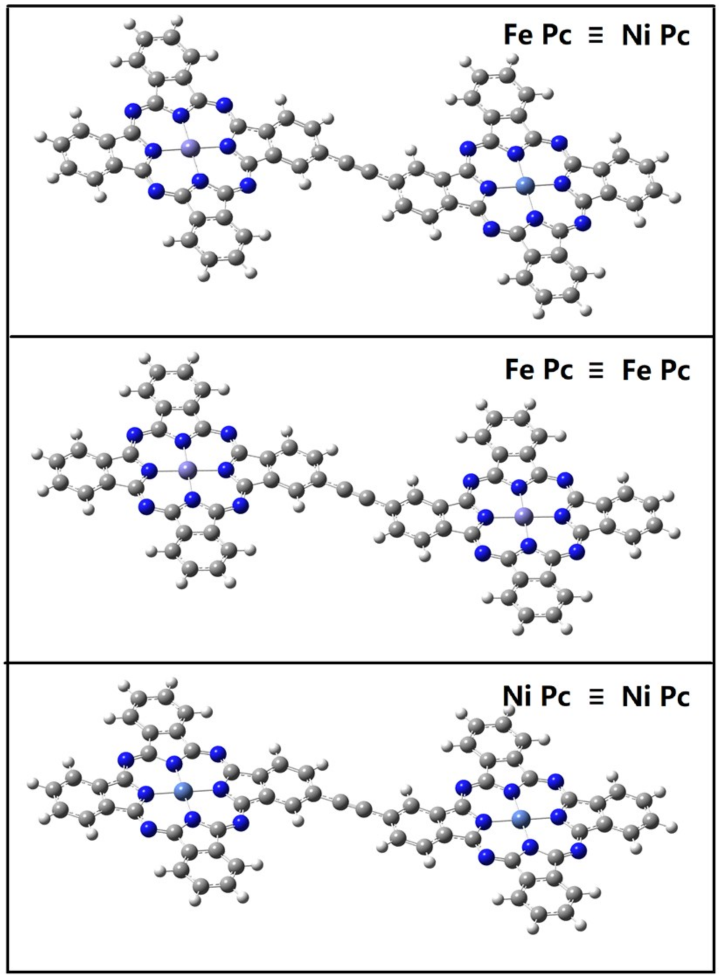

Fig. S12 Schematic structures of FePc≡NiPc, FePc≡FePc, and NiPc≡NiPc.

References

S1. W. Liu, Y. Hou, H. Pan, W. Liu, D. Qi, K. Wang, J. Jiang, X. Yao, *J. Mater. Chem. A*, 2018, **6**, 8349-8357.

S2 P.J. Stephens, F.J. Devlin, C.F. Chabalowski and M. J. Frisch, *J. Phys. Chem.*, 1994, **98**, 11623-1127.

S3 M. Ernzerhof and G. E. Scuseria, *J. Chem. Phys.*, 1999, **110**, 5029-5036.

S4 S. Grimme, J. Antony, S. Ehrlich and H. Krieg, *J. Chem. Phys.*, 2010, **132**, 154104-154119.